# Proposal for an experiment to measure the Hausdorff dimension of quantum-mechanical trajectories

H. Kröger*
*Département de Physique, Université Laval, Québec, Quebec, Canada G1K 7P4*
(Received 6 June 1995; revised manuscript received 11 September 1996)

We make a proposal for a Gedanken experiment, based on the Aharonov-Bohm effect, regarding how to measure in principle the zigzagness of the trajectory of propagation (aberration from its classical trajectory) of a massive particle in quantum mechanics. Experiment I is conceived to show that contributions from quantum paths aberrating from the classical trajectory are directly observable. Experiment II is conceived to measure average length, scaling behavior, and critical exponent (Hausdorff dimension) of quantum-mechanical paths. [S1050-2947(97)08902-6]

PACS number(s): 03.65.Bz

## I. BACKGROUND

In order to demonstrate the distinction between classical mechanics and quantum mechanics one often considers the ground-state energy of a system that has bound states. For example, for the harmonic oscillator classical and quantum-mechanical ground-state energy differ (in one space dimension) by

$$E_{\mathrm{qm}}-E_{\mathrm{cl}}=\tfrac{1}{2}\hbar\omega. \tag{1}$$

The existence of such an effect can be understood in terms of Heisenberg's uncertainty principle. But the distinction between classical and quantum mechanics does not only show up in bound states but also in scattering states. Let us consider the propagation of a massive particle. Classical mechanics predicts that the particle follows smooth (differentiable) trajectories. However, in quantum mechanics according to Feynman and Hibbs [1] the paths are nondifferentiable, self-similar curves, i.e., zigzag curves (see Fig. 1). Feynman and Hibbs noticed in 1965 the property of self-similarity, which plays an eminent role in many areas of modern physics. Mandelbrot [2] has introduced the notion of fractal geometry and pointed out that self-similarity is a characteristic feature of a fractal. Fractals are characterized by a fractal dimension $d_f$ or a Hausdorff dimension $d_H$. Abbot and Wise [3] have demonstrated by an analytic calculation that quantum-mechanical free motion yields paths that are fractal curves with Hausdorff dimension $d_H=2$. The corresponding classical system follows a trajectory with $d_H=1$ (the Hausdorff dimension $d_H$ coincides with the topological dimension $d_{\mathrm{top}}$ when the object is ''not fractal'' and $d_{\mathrm{top}}=1$ for a curve). Thus we can express the distinction between classical and quantum mechanics by the Hausdorff dimension of propagation of a free massive particle,

$$d^H_{\mathrm{qm}}-d^H_{\mathrm{cl}}=1. \tag{2}$$

For the sake of later discussions, let us recall the basic ingredients of Abbot and Wise's calculation. They consider the quantum-mechanical motion of a free particle. They assume measurements of the position of the particle at consecutive time intervals $\Delta t$. The uncertainty of position is $\Delta x$. Let us call this a monitored path. Taking a measurement means there is an interaction with the particle, hence it is no longer ''free.'' Without specifying what the interaction is, Abbot and Wise consider that the measurement implies a minimal disturbance of momentum, given by Heisenberg's uncertainty relation $\Delta p \geqslant \hbar/\Delta x$. When $\Delta x$ goes to zero, this generates an erratic path. Their calculation starts at $t=0$ from a localized $(\Delta x)$ wave packet and they compute the length as the expectation value of position at time $\Delta t$ and its scaling when $\Delta t \to 0$ and $\Delta x \to 0$. From this they deduce $d_H=2$ for an average monitored path. This result has been generalized by

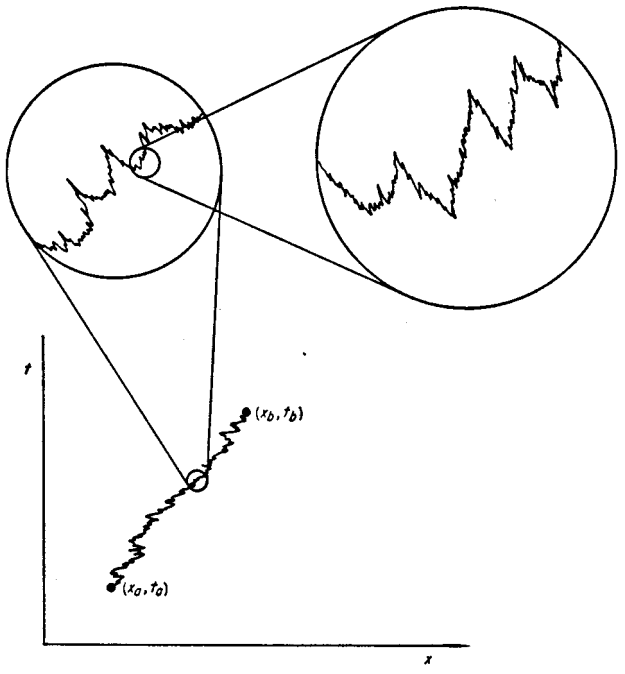


FIG. 1. Typical paths of a quantum-mechanical particle are highly irregular on a fine scale, as shown in the sketch. Thus, although a mean velocity can be defined, no mean-square velocity exists at any point. In other words, the paths are nondifferentiable. The figure is taken from Ref. [1].

*Electronic address: hkroger@phy.ulaval.ca

 © 1997 The American Physical Society

Campesino-Romeo *et al.* [4] who find $d_H=2$ for a monitored average path in the presence of a harmonic oscillator potential.

In contrast to that one can ask: What is $d_H$ for an unmonitored path? As mentioned above, the geometric characteristics of quantum paths, like zigzagness, nondifferentiability, and self-similarity have already been known to Feynman and Hibbs by 1965. It should be noted that they have also computed the essential pieces, which almost proves $d_H=2$ for an unmonitored average quantum-mechanical path. Their calculation includes the presences of any local potential. Moreover, their calculation shows the close connection with Heisenberg's uncertainty principle. So let us recall here the basic steps of Feynman and Hibbs's calculation [5]. They consider the Hamiltonian

$$H=\frac{-\hbar^2\Delta}{2m}+V(x), \tag{3}$$

where $V$ denotes a local potential. The quantum-mechanical transition element from a state $|x_{\rm in},t=0\rangle$ to a state $|x_{\rm fin},t=T\rangle$ is given by

$$\begin{aligned}\langle x_{\rm fin},t=T|x_{\rm in},t=0\rangle&=\langle x_{\rm fin}|\exp\left[-\frac{i}{\hbar}HT\right]|x_{\rm in}\rangle\\&=\int[dx(t)]\exp\left[\frac{i}{\hbar}S[x(t)]\right].\end{aligned} \tag{4}$$

The expression on the right-hand side is the path integral [1], i.e., the sum over paths $x(t)$, which start at $x_{\rm in}$ at $t=0$ and arrive at $x_{\rm fin}$ at $t=T$. The paths are ''weighted'' by a phase factor $\exp\{iS[x(t)]/\hbar\}$, where $S$ is the classical action corresponding to the above Hamiltonian for a given path,

$$S=\int_0^T dt\,\frac{m}{2}\,\dot{x}^2-V(x(t)). \tag{5}$$

Analogously, the transition element of an operator $F[\hat{x}]$ is given by

$$\begin{aligned}\langle F[\hat{x}]\rangle&=\langle x_{\rm fin},t=T|F[\hat{x}]|x_{\rm in},t=0\rangle\\&=\int[dx(t)]F[x(t)]\exp\left[\frac{i}{\hbar}S[x(t)]\right].\end{aligned} \tag{6}$$

Now suppose time is divided into small slices $\delta\,[x_i=x(t_i)]$ giving the action

$$S=\sum_{i=1}^{N-1}\delta\left[\frac{m}{2}\left(\frac{x_{i+1}-x_i}{\delta}\right)^2-V(x_i)\right]. \tag{7}$$

Feynman and Hibbs obtain the general relation

$$\left\langle\frac{\partial F}{\partial x_k}\right\rangle=-\frac{i\delta}{\hbar}\left\langle F\,\frac{\partial S}{\partial x_k}\right\rangle. \tag{8}$$

Putting $F=x_k$, this yields

$$\langle 1\rangle=\frac{i}{\hbar}\left\langle mx_k\left(\frac{x_{k+1}-x_k}{\delta}-\frac{x_k-x_{k-1}}{\delta}\right)+\delta x_kV'(x_k)\right\rangle. \tag{9}$$

In the limit $\delta\to0$, the potential term becomes negligible and one obtains

$$\left\langle m\,\frac{x_{k+1}-x_k}{\delta}\,x_k\right\rangle-\left\langle x_km\,\frac{x_k-x_{k-1}}{\delta}\right\rangle=\frac{\hbar}{i}\langle 1\rangle. \tag{10}$$

This means the transition element of a product of position and momentum depends on the order in time of these two quantities. This leads to the usual operator commutation law between position and momentum, which implies the Heisenberg uncertainty relation between position and momentum. Now suppose one advances the second term on the left-hand side of Eq. (10) by one time slice $\delta$

$$\left\langle x_km\,\frac{x_k-x_{k-1}}{\delta}\right\rangle=\left\langle x_{k+1}m\,\frac{x_{k+1}-x_k}{\delta}\right\rangle+O(\delta). \tag{11}$$

Then in the limit $\Delta t\equiv\delta\to0$, Eqs. (10) and (11) imply

$$\begin{aligned}\langle(x_{k+1}-x_k)^2\rangle&=-\frac{\hbar\delta}{im}\langle 1\rangle.\\\langle(\Delta x)^2\rangle&\propto\frac{\hbar}{m}\,\Delta t.\end{aligned} \tag{12}$$

This is Feynman and Hibbs's important result on the scaling relation between a time increment $\Delta t$ and the corresponding average length increment of a typical quantum path. Now we make an assumption that we consider as plausible, but that we were not able to prove:

$$\langle|\Delta x|\rangle^2=\langle(\Delta x)^2\rangle. \tag{13}$$

Now let us consider a finite time interval $T=N\Delta t$ and the length of the path the particle has traveled between $x_0=x(t_0)=x_{\rm in}$ and $x_N=x(t_N)=x_{fi}$. Classically the length is given by

$$L_{\rm class}=\sum_{k=0}^{N-1}|x_{k+1}-x_k|. \tag{14}$$

According to Feynman and Hibbs, the corresponding quantity in quantum mechanics is the transition element given by Eq. (6), where $F[\hat{x}]$ is given by the classical length,

$$\begin{aligned}\langle L\rangle&=\left\langle x_{\rm fin},t=T\left|\sum_{k=0}^{N-1}|x_{k+1}-x_k|\right|x_{\rm in},t=0\right\rangle\\&=\int[dx(t)]\sum_{k=0}^{N-1}|x(t_{k+1})-x(t_k)|\exp\left[\frac{i}{\hbar}S[x(t)]\right].\end{aligned} \tag{15}$$

One should note that this is not an expectation value in the usual sense. Feynman and Hibbs refer to the transition elements as ''weighted averages.'' The weighting function in quantum mechanics is a complex function. Thus the transition element is in general complex. Using Eqs. (12) and (13) one computes

$$\langle L\rangle = N\langle|\Delta x|\rangle = \frac{T}{\Delta t}\,\langle|\Delta x|\rangle \propto \frac{T\hbar}{m\langle|\Delta x|\rangle}. \tag{16}$$

Comparing this with the definition of the Hausdorff dimension [see Eqs. (17) and (18)] and putting $\epsilon=\langle|\Delta x|\rangle$ yields Hausdorff dimension $d_H=2$ for an unmonitored typical quantum-mechanical path in the presence of an arbitrary local potential.

Because the rigor of this result hinges upon the validity of the assumption in Eq. (13) it is interesting to check this result by a numerical calculation. Kröger *et al.* [6] have computed the transition element of the path length $\langle L\rangle = \langle \sum_{k=0}^{N-1}|x_{k+1}-x_k|\rangle$ via numerical simulations of the path integral on a time lattice, however, using imaginary time (in order to be able to use Monte Carlo methods). The results for the Hausdorff dimension of unmonitored paths are compatible with $d_H=2$ for free motion.

When we ask what is the Hausdorff dimension for a quantum mechanical particle with interaction, we expect for local potentials via Feynman and Hibbs' calculation to obtain the value $d_H=2$. The numerical simulations by Kröger *et al.* [6] in the presence of local potentials such as the harmonic oscillator or Coulomb potential give results also compatible with $d_H=2$. However, $d_H\neq 2$ has been found in the case of velocity-dependent interactions. More precisely, for velocity-dependent interactions $U\sim U_0|\dot{x}|^{\alpha}$, the value $d_H=2$ has been found for $\alpha\leqslant 2$, but $d_H<2$ for $\alpha>2$. Velocity-dependent actions play a role in condensed matter physics: The propagation in a solid medium introduces higher-order velocity terms via dispersion relations [7]. Also Brueckner's [8] theory of nuclear matter saturation introduces velocity-dependent interactions. The action relevant for this work, namely, the interaction of a massive charged particle with a vector potential, is also a velocity-dependent action, being linear in the velocity ($\alpha=1$). Thus one expects also $d_H=2$.

Let us summarize the present situation concerning the fractal dimension of an average quantum path in the presence of a local potential: A monitored path is a path where measurements of position are taken at some discrete time intervals; i.e., the particle undergoes interaction. Possible ways to do this are discussed in Sec. III. On the other hand an unmonitored path is undisturbed by interaction (in nonrelativistic quantum mechanics we neglect interaction with the vacuum, particle creation, vacuum polarization, etc.). There is a rigorous proof of $d_H=2$ for monitored paths. For unmonitored paths, there is strong indication that $d_H=2$ holds also. However, neither a rigorous proof nor a numerical simulation in real time has been established so far. One might ask: What is the relationship between monitored and unmonitored paths and why should $d_H$ coincide for both? First of all, the operational definition of length employed is different. For monitored paths, the authors of Refs. [3, 4] have defined length $\Delta l$ as the usual quantum-mechanical expectation value of the absolute value of an increment of position in the state of a wave function having been evolved for an increment of time $\Delta t$ from an original wave function being characterized by localization uncertainty $\Delta x$. In this work and Ref. [6] we are interested in the length of unmonitored paths, however, not in length corresponding to an infinitesimal time interval, but the length corresponding to a finite time interval, say $T$. This involves a number of intermediate times. The goal to seek information on the average of an observable at several times leads to Feynman and Hibbs' transition element, which we have employed here. Thus the length definition and average are different. However, there is a common link, which may be considered as the physical origin of fractal paths: Heisenberg's uncertainty relation and behind this the fundamental commutator relation between position and momentum. For the case of the monitored paths, the process of localization leads via the uncertainty principle to erratic paths. But also for the case of unmonitored paths, Feynman and Hibbs's calculation shows that the scaling relation between $\Delta x$ and $\Delta t$, Eq. (12), is directly related to the commutator relation between position and momentum, which again is directly related to the uncertainty principle. But why then should the outcome of $d_H$ agree? Because the result $d_H=2$ for unmonitored paths is not rigorously established yet, one can only speculate on this hypothetical coincidence. For unmonitored paths the scaling relation Eq. (12) is valid for a very large class of interactions, namely, all local potentials. Also the numerical simulations in Ref. [6] have given, within statistical errors, $d_H=2$ for all local potentials investigated. In other words there is an indication (not a proof) that $d_H=2$ for unmonitored paths in the presence of arbitrary local potentials. On the other hand, monitoring a path means interaction by measurement. If one assumes that such interaction is described by a local potential it seems plausible that $d_H$ coincides for monitored and unmonitored paths.

If the zigzagness of quantum paths is such a fundamental property of quantum mechanics, one might ask if it has been measured experimentally. To the author's knowledge such an experiment has not been done yet. Thus the central theme of this work is made up of the following questions: Can we observe experimentally the zigzagness of quantum-mechanical trajectories? Is such an experiment feasible in principle? Can it be done in practice? The motivation is twofold: (a) Zigzagness of paths is a fundamental property of quantum mechanics, and thus it would be desirable to have a direct experimental evidence. (b) As we have mentioned above, there is an indication that velocity-dependent interactions may change the Hausdorff dimension. Thus an experiment measuring the Hausdorff dimension would yield information on the interaction.

The zigzagness of the free quantum-mechanical motion is principally not measurable, because every measurement involves an interaction with the system. Hence the system is no longer free. Thus we can study at best the quantum-mechanical motion of an interacting particle. As our numerical simulations have shown, one would still expect a zigzag motion. For a certain class of potentials (local potentials) the fractal dimension would be the same as for free motion. What do we want to measure, in particular? We want to measure the geometry of the average quantum-mechanical trajectory, in particular we want to measure the average

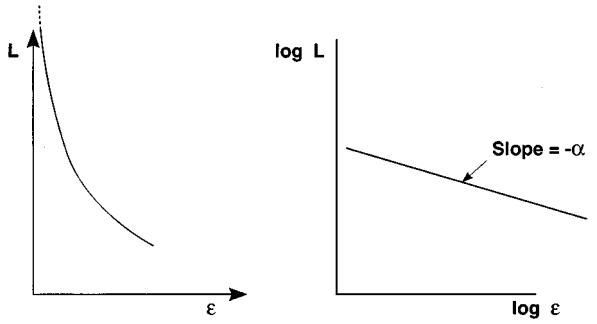


FIG. 2. Graph corresponding to Eq. (17). Length vs $\epsilon$. The log-log plot allows one to determine the critical exponent $\alpha$.

length of the trajectories, then the scaling of this length under variation of an elementary length scale, and finally extract a critical exponent, which is closely related to the fractal dimension (Hausdorff dimension) of the trajectory.

## II. REMINDER ON FRACTAL DIMENSION

A definition of the Hausdorff (fractal) dimension $d_H$ is given by Mandelbrot [2]. He considers as an example how to measure the length of the coastline of England. One takes a yardstick, representing a straight line of a given length. Let $\epsilon$ denote the ratio of the yardstick length to a fixed unit length. Then one walks around the coastline, and measures the length of the coast with the particular yardstick (starting a new step where the previous step leaves off). The number of steps multiplied with the yardstick length (characterized by $\epsilon$) gives a value $L(\epsilon)$ for the coastal length. Then one repeats the same procedure with a smaller yardstick, say $\epsilon'$. Doing this for many values of $\epsilon$ yields a function $L$ versus $\epsilon$. It has qualitatively the shape shown in Fig. 2. One observes for a wide range of length scales $\epsilon$ that the length of the British coast obeys a power law

$$L(\epsilon)=L_0\epsilon^{-\alpha}. \tag{17}$$

This looks like the critical behavior of a macroscopic observable at the critical point, thus $\alpha$ is called a critical exponent. The Hausdorff dimension $d_H$ is defined by

$$\alpha=d_H-1. \tag{18}$$

So, one has an elementary length scale $\epsilon$, and one measures the length of the curve $L(\epsilon)$. Then $\epsilon$ goes to zero. One looks for a power-law behavior (critical behavior) and determines the critical exponent. The Hausdorff dimension is directly related to the critical exponent.

## III. MEASUREMENT OF POSITION IN QUANTUM MECHANICS AND ELEMENTARY LENGTH

In the calculation of the Hausdorff dimension for unmonitored paths in Sec. I, one has discretized time with an increment $\Delta t$. The average increment of length $\langle|\Delta x|\rangle$ and the average total length $\langle L\rangle$ have been determined dynamically by the system. One has found a power law $\langle L\rangle\sim L_0\langle|\Delta x|\rangle^{-\alpha}$ and the critical exponent $\alpha$ has been extracted in the limit $\langle|\Delta x|\rangle\to 0$, which is equivalent to $\Delta t\to 0$, due to the scaling relation (12). In an experiment, in order to measure the length $\langle L\rangle$ and extract the critical exponent one would proceed differently: One would introduce an elementary length scale $\Delta x_{\rm exp}$ at the disposal of the experimentator. Then one would measure the length $\langle L\rangle$ by sequential measurements of position as a function of $\Delta x_{\rm exp}$; i.e., one would monitor the path. Again one would expect a power law $\langle L\rangle\sim L_0'\langle\Delta x_{\rm exp}\rangle^{-\alpha'}$. Then one would approach the limit $\Delta x_{\rm exp}\to 0$. One would expect for the critical exponent $\alpha'=\alpha$. A typical quantum-mechanical path is sketched in Fig. 3. Zigzag motion occurs in the transversal as well as in the longitudinal direction (not shown in Fig. 3).


FIG. 3. Schematic plot of propagation of massive free particle. Dashed line: classical trajectory. Full line: quantum-mechanical zigzag motion. Note: there is zigzagness in all spatial dimensions, i.e., in longitudinal as well as transversal directions.

We have to say what we mean by elementary length (''yardstick''). From the experimental point of view it means the length scale of experimental resolution when measuring position. In the following we give several examples of how this can be done: (a) Sequence of absorbers (screens), each with a slit [Fig. 4(a)]. Here the elementary length $\Delta x$ is given by the distance between the slits. (b) Spark wire chamber [Fig. 4(b)]. Here the elementary length $\Delta x$ is given by the distance between the wires. (c) Bubble chamber. Here the elementary length $\Delta x$ is given by the spatial resolution of two different bubbles. In the experimental proposal presented below we will use neither of those, but we will consider as an elementary length the distance between neighboring solenoids carrying magnetic flux because the suggested experiment is a generalized Aharonov-Bohm experiment.

How could one measure the length of a typical quantum path by monitoring the position? In principle, this can be done by a setup of an electron source, a detector, and multiple screens with multiple holes [see Figs. 5(a) and 5(b)]. In order to measure by which hole an electron has passed, Feynman and Hibbs [1] have suggested two possible experiments: (a) A light source is placed behind the screen [Fig. 5(a)]. One observes scattering of light from the electron through one of the holes. From the scattered light one can determine by which holes the electron has passed. (b) As an alternative, one can arrange such that the screen with holes can move freely in a vertical direction [Fig. 5(b)]. Before the electron passes, the screen is at rest. When the electron passes, it scatters from the screen at the hole. The hole by which the electron passes can be determined by measuring if the screen is recoiling upward or downward, i.e., by measuring the momentum of the screen. One can imagine placing several such screens, each carrying several holes. Then one determines the holes that the electron has passed and clocks the time for each passage of a hole, in order to determine if there has been forward movement from the source to the detector.

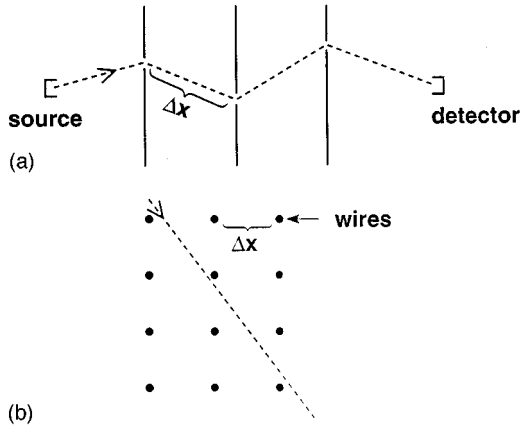


FIG. 4. Measurement of position and definition of elementary length scale $\Delta x$. (a) Sequence of screens with holes. (b) Wire chamber.

The experimental length resolution $\Delta x$ is given by the distance between neighboring screens and the distance between holes on a screen. We want to determine the length of the path. In order to extract a fractal dimension we need to study $\Delta x \to 0$. Then we run into the following problems: The

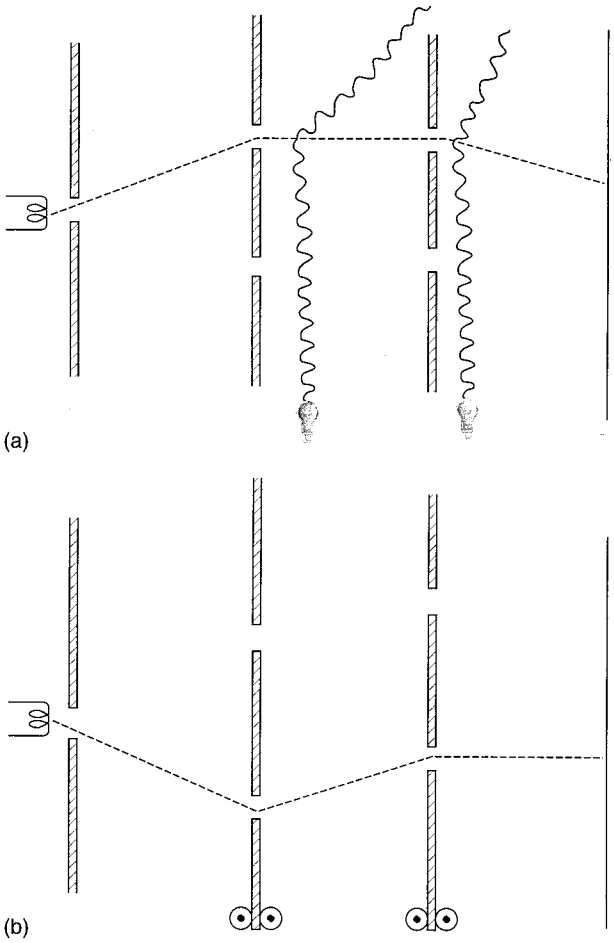


FIG. 5. Measurement of position of holes traversed by an electron. (a) Determination of position by electron-light scattering. (b) Determination of position by measuring recoil direction and momentum of movable screen.

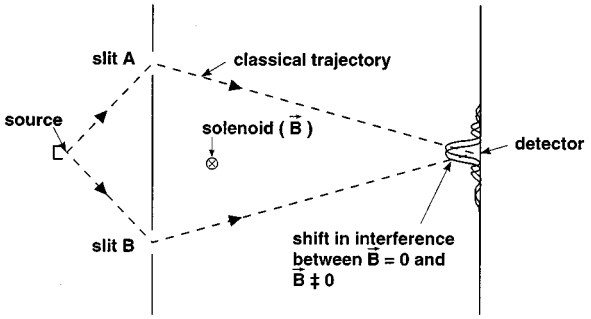


FIG. 6. Setup of Aharonov-Bohm experiment. A charged particle (electron) is scattered from two slits and one observes interference in the detector. When placing a solenoid (thin magnetic flux tube) in the region between the classical trajectories, one observes a shift in interference.

first one is a kind of technical problem: When we put more screens between source and detector, then fewer electrons will arrive at the screen. The counting rate goes down quite drastically. This can be compensated by a longer beam time, i.e., by emitting more electrons. There is, however, another more serious problem. Consider alternative (a): In order to tell if an electron has passed by a particular hole, the electron is scattered from light with wavelength $\lambda$. The (scattering) source of light of wavelength $\lambda$ cannot be located in space with precision greater than order of $\lambda$. Thus when we want to decrease the spatial resolution $\Delta x$, we need to decrease the wave length $\lambda$ accordingly. Light carries a momentum $2\pi\hbar/\lambda$, which is (partially) transferred to the electron. Thus the smaller $\Delta x$, the larger the momentum transferred to the electron and the more the original quantum path of the electron is altered. This is Heisenberg's uncertainty principle: Any determination of the alternative (sequence of holes) taken by a process capable of following more than one alternative destroys the interference between alternatives. In other words, when we determine by which holes the electron has passed, then the final interference pattern no longer has the shape shown in Fig. 6 (this has nothing to do with the fact that there are several screens; it happens also for one screen with two holes).

For this reason, we are going to suggest below an experiment without monitoring the path. The experiment is different in the following sense: We do not place screens, so there is no loss in the counting rate. Secondly, our proposal is based on the Aharonov-Bohm effect, which is classically a null effect, contrary to the above setup with screens, which classically does not give a null effect. Finally, in our proposal we determine the path via the topology of the Aharonov-Bohm effect.

## IV. REMINDER ON AHARONOV-BOHM EXPERIMENT

The experiments we will suggest in the next sections are generalizations of the Aharonov-Bohm effect. Thus it is worthwhile to recall the notion of the Aharonov-Bohm effect and the experimental setup, which has confirmed this effect. Aharonov and Bohm [9] have suggested in 1959 that there should be an observable difference between classical and quantum mechanics when a charged particle interacts with a magnetic field. In particular, when the magnetic field (ideal-

ized) corresponds to an infinitely long, infinitesimally thin flux tube (solenoid), then outside of the flux tube the magnetic field $\vec{B}=0$, but the vector potential is nonzero ($A_\theta \propto 1/r$ in spherical coordinates). Due to the particular geometry of the magnetic field, which is independent of the $z$ coordinate (the flux tube is assumed to be parallel to the $z$ axis), we have an effective two-dimensional (2D) system in any plane perpendicular to the flux tube.

Now consider a charged particle (charge $q$) passing by (scattering from) the solenoid. Classically, the Lorentz force is zero. But quantum mechanically, the electron wave function is affected by the nonvanishing vector potential. Aharonov and Bohm [9] have computed the cross section for scattering from an infinitesimally thin flux tube with flux $\phi$. Choosing the gauge of the vector potential such that the vector potential takes the form

$$A_r=0, \quad A_\theta=\phi/2\pi r, \tag{19}$$

they find the cross section (in the notation of Ref. [10])

$$\frac{d\sigma}{d\theta}=\frac{1}{2\pi k}\frac{\sin^2(\pi\alpha)}{\sin^2(\theta/2)}, \quad \alpha=\frac{q\phi}{2\pi\hbar c}, \tag{20}$$

where $k$ is the wave number.

The Aharonov-Bohm effect has been confirmed by experiment [11]. The setup corresponds to a two-slit interference experiment (see Fig. 6). A very thin solenoid is placed perpendicular to the plane in the region between the two slits and the detector (region between the two classical trajectories). Then the interpretation is as follows [12]. One compares two cases: (a) The solenoid is turned off (flux and vector potential are zero). Then there is interference due to scattering from two sources. This is due to a difference in the phase of the wave function $\delta(\vec{B}=0)$, corresponding to the two trajectories. (b) The solenoid is turned on (flux and vector potential are nonzero.) Then quantum mechanics says that the wave function experiences a change of phase due to the presence of the vector potential given by

$$\delta=\delta(\vec{B}=0)+\frac{q}{\hbar c}\int_C d\vec{l}\cdot\vec{A}, \tag{21}$$

where $C$ denotes the closed curve formed by the two trajectories, $S$ is the area of the interior of this curve, $\vec{A}$ is the vector potential, $\vec{B}$ is the magnetic field, $\phi$ is the magnetic flux, and $q$ is the charge of the particle. Thus the phase change of the interference amplitude due to the presence of the vector potential is basically given by the flux through the region $S$,

$$\Delta\delta=\delta-\delta(\vec{B}=0)=\frac{q}{\hbar c}\int_C d\vec{l}\cdot\vec{A}=\frac{q}{\hbar c}\int_S d\vec{s}\cdot\vec{B}=\frac{q\phi}{\hbar c}. \tag{22}$$

This change of phase $\Delta\delta$ shifts the maximum of the interference pattern (see Fig. 6). Again, classically there is no such effect, because the magnetic field is practically zero (exactly zero for an idealized solenoid) outside of the solenoid and hence everywhere on the classical trajectory. In summary, the Aharonov-Bohm effect shows that there is a difference between quantum mechanics and classical mechanics, and moreover, the vector potential is a real physical quantity.

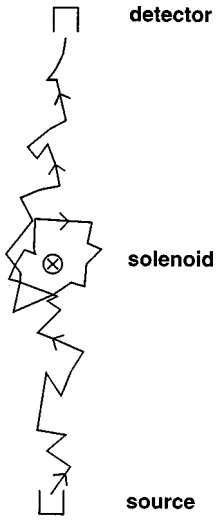


FIG. 7. Schematic quantum path from source to detector winding around solenoid.

In the Aharonov-Bohm experiment, as described above the quantum effects come from the phase change of the wave function due to the presence of the vector potential. In order to better understand the experiment suggested below, we need to take a closer look into the quantum mechanics of the Aharonov-Bohm effect. It actually turns out that the above explanation in terms of phase change of the wave function is valid only in the case when the distance $h$ between the solenoid and the classical trajectories (see Fig. 6) is large compared to the de Broglie wavelength $\lambda$. Note that the classical region is given by $\Delta x \gg \hbar/p=\lambda/2\pi$, and the region of quantum mechanics is given by $\Delta x \ll \hbar/p=\lambda/2\pi$. In general, the presence of the vector potential creates a phase change plus a change of modulus of the wave function. This is so, in particular, when one of the classical trajectories is close to the solenoid. This is just the situation, which will play an important role in our experimental proposal.

Schulman [13] was the first to point out the connection between quantum mechanics and topology in the Aharonov-Bohm effect. This holds in the strict sense only in the idealized situation of an infinitely thin and long flux tube. Quantum paths can go by either to the left or to the right side of the solenoid. Mathematically, this is equivalent to a plane with a hole at the position of the solenoid. Quantum-mechanical propagation proceeds forward in time but forward and backward in both space dimensions (zigzag trajectories). Thus paths can occur, which wind around the solenoid (see Fig. 7). The classical Hamiltonian in the presence of the vector potential is given by

$$H=\frac{1}{2m}\left(\vec{p}-\frac{q}{c}\vec{A}\right)^2, \tag{23}$$

and the action is given by

$$S=\int dt\,\frac{m}{2}\dot{\vec{x}}^2+\frac{q}{c}\dot{\vec{x}}\cdot\vec{A}(\vec{x},t). \tag{24}$$

Thus, when considering quantization by path integral, Eq. (6), there occurs an Aharonov-Bohm phase factor due to the vector potential present in the action. This factor is $\exp[i\alpha(\theta_{\rm fin}-\theta_{\rm in}+2\pi n_w)]$ [see Eq. (29) below], when the path winds $n_w=0,\pm1,\pm2,\ldots$ times around the solenoid, and $\alpha=q\phi/2\pi\hbar c$. This factor depends only upon the initial and final azimuthal angle $\theta$ and the number of windings, but otherwise it is independent of the path. In other words, paths can be classified by their winding number; they fall into homotopy classes.

Now let us consider the Aharonov-Bohm propagator. Fortunately, this expression can be computed analytically. We follow the presentation by Wilczek [10]. The idea is to start from the free propagator, and decompose it into classes corresponding to winding numbers $n_w=0,\pm1,\pm2,\ldots,\pm\infty$. Then one takes the free propagator in each winding class, multiplies it by the Aharonov-Bohm phase factor, and finally sums over all windings. The free propagator in $D=2$ dimensions is given by (see Ref. [14])

$$\begin{aligned}K^{\rm free}&=\langle\vec{x}_{\rm fin}|\exp[-iHT/\hbar]|\vec{x}_{\rm in}\rangle\\&=\frac{\mu}{2\pi i\hbar T}\exp\left[\frac{i\mu}{2\hbar T}(\vec{x}_{\rm fin}-\vec{x}_{\rm in})^2\right]\\&=\frac{\mu}{2\pi i\hbar T}\exp\left[\frac{i\mu}{2\hbar T}[r'^2+r^2-2r'r\cos(\theta'-\theta)]\right].\end{aligned}\tag{25}$$

In order to avoid confusion with the magnetic quantum number $m$, the particle mass is denoted by $\mu$ in the following.

Now one allows $\theta'$ and $\theta$ to correspond to different winding number sectors. One defines $\Theta=\theta'-\theta+2\pi n_w$. The free propagator is periodic in $\theta$ between $-\pi$ and $\pi$. Then one defines $\tilde{K}^{\rm free}(\lambda)$ by Fourier transformation of $K^{\rm free}(\theta)$,

$$\begin{aligned}\tilde{K}^{\rm free}(\lambda)&=\int_{-\pi}^{+\pi}\frac{d\theta}{2\pi}\exp[-i\lambda\theta]K^{\rm free}(\theta)\\&=\int_{-\pi}^{+\pi}\frac{d\theta}{2\pi}\frac{\mu}{2\pi i\hbar T}\\&\quad\times\exp\left[\frac{i\mu}{2\hbar T}[r'^2+r^2-2r'r\cos(\theta)]\right]\\&=\frac{\mu}{2\pi i\hbar T}\exp\left[\frac{i\mu}{2\hbar T}(r'^2+r^2)\right]I_{|\lambda|}\left(\frac{\mu rr'}{i\hbar T}\right),\end{aligned}\tag{26}$$

where $I_v(z)$ is the modified Bessel function. Thus the free propagator in the winding sector $n_w$ is given by

$$\begin{aligned}K^{\rm free}_{n_w}(\Theta)&=\int_{-\infty}^{+\infty}d\lambda\ \exp[i\lambda\Theta]\tilde{K}^{\rm free}(\lambda)\\&=\int_{-\infty}^{+\infty}d\lambda\ \exp[i\lambda(\theta'-\theta+2\pi n_w)]\frac{\mu}{2\pi i\hbar T}\\&\quad\times\exp\left[\frac{i\mu}{2\hbar T}(r'^2+r^2)\right]I_{|\lambda|}\left(\frac{\mu rr'}{i\hbar T}\right).\end{aligned}\tag{27}$$

The total free propagator, being the sum over all windings is then

$$\begin{aligned}K^{\rm free}(r',\theta';r,\theta)&=\sum_{n_w=-\infty}^{+\infty}\int_{-\infty}^{+\infty}d\lambda\ \exp[i\lambda(\theta'-\theta+2\pi n_w)]\frac{\mu}{2\pi i\hbar T}\exp\left[\frac{i\mu}{2\hbar T}(r'^2+r^2)\right]I_{|\lambda|}\left(\frac{\mu rr'}{i\hbar T}\right)\\&=\sum_{m=-\infty}^{+\infty}\exp[im(\theta'-\theta)]\frac{\mu}{2\pi i\hbar T}\exp\left[\frac{i\mu}{2\hbar T}(r'^2+r^2)\right]I_{|m|}\left(\frac{\mu rr'}{i\hbar T}\right).\end{aligned}\tag{28}$$

This is the free propagator, as given by Eq. (25), expressed in a more complicated way. However, now it is easy to write down the Aharonov-Bohm propagator. The Aharonov-Bohm propagator is the sum over all paths, where each path is weighted with the phase $\exp[iS/\hbar]$. The paths can be decomposed into classes with a given winding number $n_w$, where $n_w=0,\pm1,\pm2,\ldots$. Thus the Aharonov-Bohm propagator for a given winding number $n_w$ is just the free propagator for winding number $n_w$ times the Aharonov-Bohm phase factor. For the vector potential given by Eq. (19), this phase factor given by

$$\exp\left[\frac{i}{\hbar}\int_0^T dt\,\frac{q}{c}\dot{\vec{x}}\cdot\vec{A}\right]=\exp\left[\frac{iq}{\hbar c}\int_{x_{\rm in}}^{x_{\rm fin}}d\vec{x}\cdot\vec{A}\right]=\exp[i\alpha(\theta'-\theta+2\pi n_w)].\tag{29}$$

Thus one finds the Aharonov-Bohm propagator for winding number $n_w$:

$$K^{\rm AB}_{n_w}(\Theta)=\int_{-\infty}^{+\infty}d\lambda\ \exp[i(\lambda+\alpha)\Theta]\tilde{K}^{\rm free}(\lambda).\tag{30}$$

The total Aharonov-Bohm propagator is finally given by

$$K^{\rm AB}(r',\theta';r,\theta)=\sum_{n_w=-\infty}^{+\infty}\int_{-\infty}^{+\infty}d\lambda\ \exp[i(\lambda+\alpha)(\theta'-\theta+2\pi n_w)]\tilde{K}^{\rm free}(\lambda)=\sum_{m=-\infty}^{+\infty}\exp[im(\theta'-\theta)]\tilde{K}^{\rm free}(\lambda-\alpha)$$

$$= \sum_{m=-\infty}^{+\infty} \exp[im(\theta'-\theta)] \frac{\mu}{2\pi i\hbar T} \exp\left[\frac{i\mu}{2\hbar T}(r'^2+r^2)\right] I_{|m-\alpha|}\left(\frac{\mu r r'}{i\hbar T}\right). \tag{31}$$

The Aharonov-Bohm propagator, when letting $r'$, $r\to\infty$ yields the Aharonov-Bohm differential cross section given by Eq. (20) (see Ref. [10]). Inspection of the free propagator and the Aharonov-Bohm propagator show the following structure: Apart from a common dimensionful prefactor $\mu/2\pi i\hbar T$, they are both functions of dimensionless arguments $\mu(r'^2+r^2)/2\hbar T$ and $\mu r' r/\hbar T$. The Aharonov-Bohm propagator further depends on the dimensionless quantity $\alpha=q\phi/2\pi\hbar c$. When we consider $r'=r$ large, then we have velocity $v=(r'+r)/T$, momentum $p=\mu v$, and the de Broglie wavelength $\lambda=2\pi\hbar/p=\pi\hbar T/\mu r$. Then the dimensionless argument of the exponential function and the Bessel function becomes $\pi r/\lambda$.

As mentioned above, the interpretation of the Aharonov-Bohm interference experiment is based on the phase change of the wave function, making the assumption that the solenoid is far away from the classical trajectories. Because we have the exact expression for the Aharonov-Bohm propagator at hand, we are able to test this assumption. We introduce a semiclassical propagator, defined by the product of the free propagator multiplied with the Aharonov-Bohm phase factor computed along the classical trajectory (straight line between $x_{\rm in}$ and $x_{\rm fin}$, zero winding)

$$K^{\rm semiclass}(r',\theta';r,\theta)=K^{\rm free}(r',\theta';r,\theta)\exp[i\alpha(\theta'-\theta)]. \tag{32}$$

Firstly, we have tested the free propagator expansion in terms of Bessel functions. We have compared the exact expression, Eq. (25), with the expansion in the magnetic quantum number $m$, Eq. (28). We have imposed a cutoff $m_{\rm max}$, letting the sum run over $-m_{\rm max}\leqslant m\leqslant m_{\rm max}$. We have kept fixed the values of parameters $\hbar=1$, $x_{\rm in}$, $x_{\rm fin}$, $L=2$, $T=10$, $\mu=1$. $L$ is the length of a straight line between $x_{\rm in}$ and $x_{\rm fin}$, which is the trajectory of classical propagation. We have chosen the origin (of spherical coordinates) to be located at some distance $h$ from the trajectory of classical propagation and equidistant from $x_{\rm in}$ and $x_{\rm fin}$. We have varied $h$ from 0 to 10 and $m_{\rm max}$ from 5 to 15. The reference value, Eq. (25), is independent from $h$ and $m_{\rm max}$. It has the value $K^{\rm free}=0.00316129-i0.0155982$. This set of parameters corresponds to the de Broglie wavelength $\lambda=10\pi$. If we identify the distance $h$ of the origin with the resolution $\Delta x$, then we cross at $h=5$ from the quantum-mechanical region to the classical region. Figure 8(a) shows the real part; Fig. 8(b) corresponds to the imaginary part. One observes rapid convergence in $m_{\rm max}$.

We have tested the assumption on the asymptotic behavior of the Aharonov-Bohm propagator by evaluating numerically the Aharonov-Bohm propagator and the semiclassical propagator. We have chosen the parameters as in Fig. 8; now we have varied $h$ and $\alpha$. The results are plotted in Figs. 9 and 10. Figure 9(a) shows the real part of the semiclassical propagator, Eq. (32). Figure 9(b) shows the real part of the Aharonov-Bohm propagator, Eq. (31). Here we have chosen the cutoff $m_{\rm max}=50$. From the convergence test of the free propagator, we estimate that $m_{\rm max}=20$ should be sufficient to guarantee stability in the sixth significant decimal digit when $h\leqslant 10$. The absolute value of the real part of the difference between the semiclassical and Aharonov-Bohm propagator is displayed in Fig. 9(c). The corresponding results for the imaginary part are plotted in Fig. 10. As in Fig. 8, this set of parameters corresponds to the de Broglie wavelength $\lambda=10\pi$ and the crossing of the quantum-mechanical region to the classical region occurs at $h=5$. One observes that when the distance $h$ becomes large, the difference between the

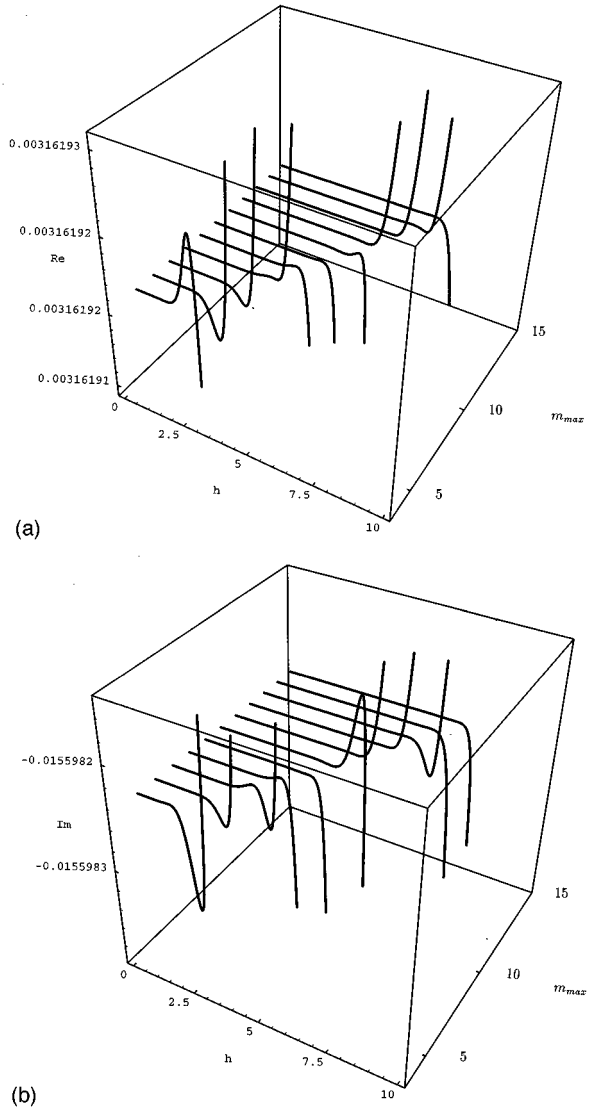


FIG. 8. Free propagator. A comparison of exact result, Eq. (25), with expansion in Bessel functions, Eq. (28). (a) Real part as function of distance $h$ from classical path and of cutoff $m_{\rm max}$, $5\leqslant m_{\rm max}\leqslant 15$. (b) Same for imaginary part. For other parameters see text.

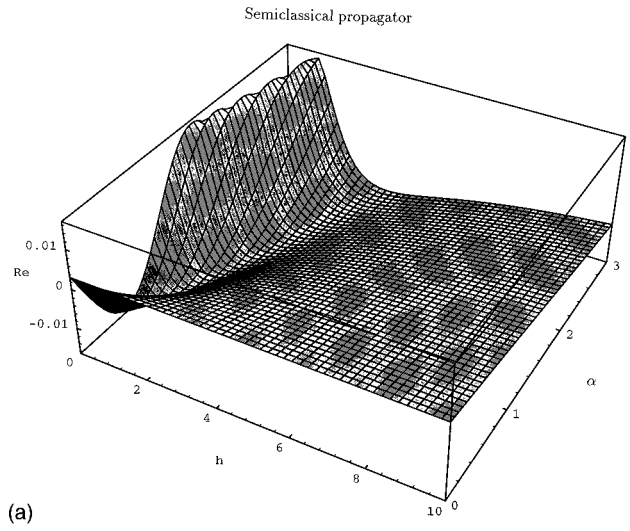


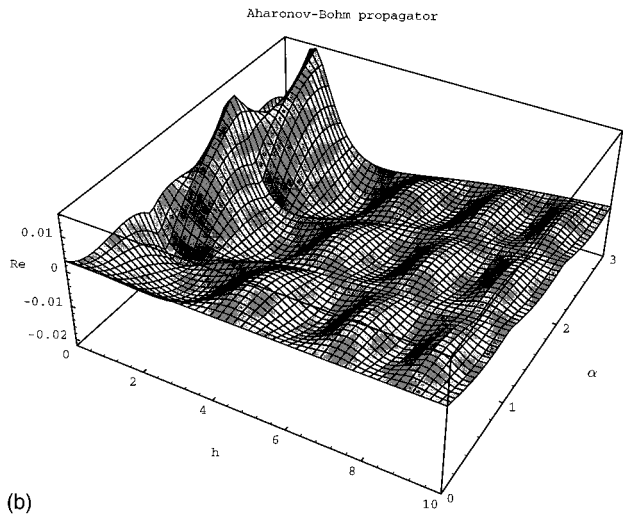


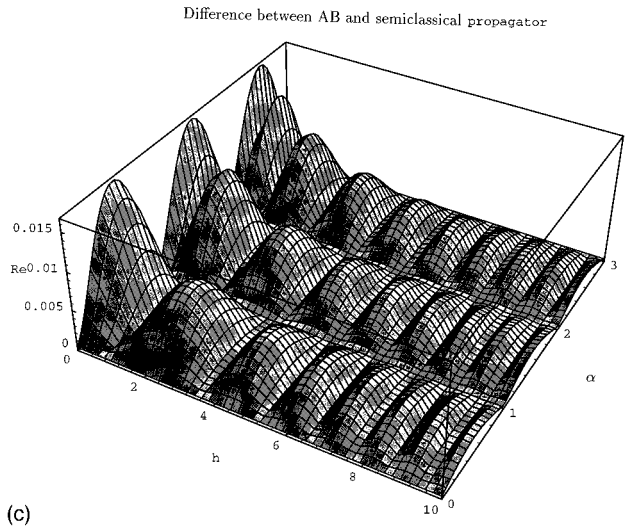


FIG. 9. (a) Real part of semiclassical propagator, Eq. (32). (b) Real part of Aharonov-Bohm propagator, Eq. (31). (c) Absolute value of the difference of both. Dependence on distance $h$ and on $\alpha$. Other parameters as in Fig. 8, cutoff $m_{\max}=50$.

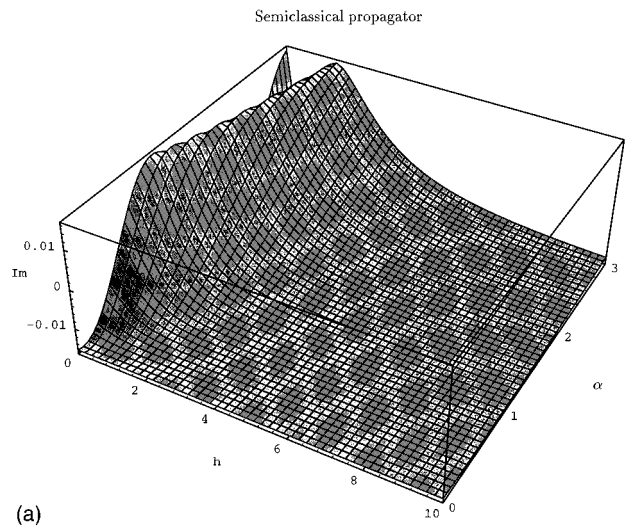


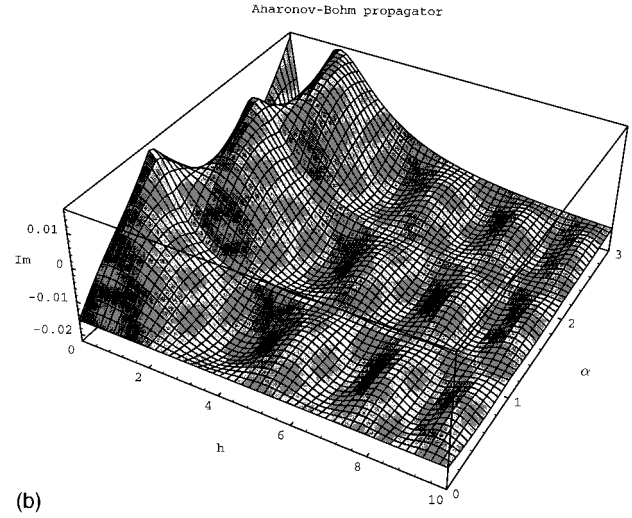


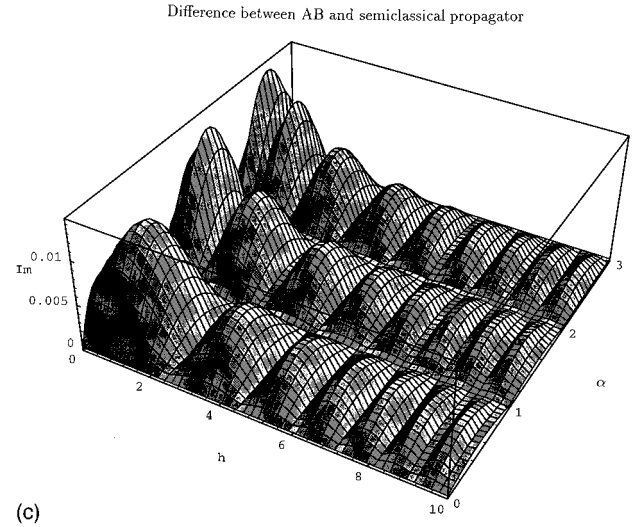


FIG. 10. Same as Fig. 9, but for the imaginary part.

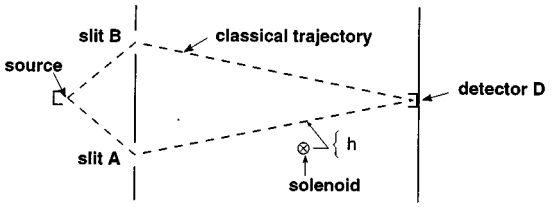


FIG. 11. Setup of Gedanken experiment I. Similar to Aharonov-Bohm experiment, but the solenoid is placed outside the region bounded by the classical trajectories.

Aharonov-Bohm propagator and the semiclassical propagator tends to zero. Moreover, one observes that the difference between these propagators is most pronounced for small distance $h$ $(h\rightarrow 0)$.

## V. GEDANKEN EXPERIMENT I TO SEARCH FOR ABERRATION FROM CLASSICAL PATH IN QUANTUM-MECHANICAL TRAJECTORIES

Now I want to suggest a Gedanken experiment in order to show that not only is there a difference between classical and quantum mechanics, but that quantum effects come from the zigzagness of quantum-mechanical trajectories. The setup is based on the Aharonov-Bohm experiment. But there is some modification. Contrary to the original experiment, where the solenoid was placed in the interior (center) of the region bounded by the two classical trajectories, now I suggest placing the solenoid in the region outside (see Fig. 11). Let $h$ denote the distance of the solenoid from the classical trajectory $A-D$. Then we let the solenoid approach the classical trajectory $(h\rightarrow 0)$. Again we consider the case (a) when the solenoid is turned off and (b) when the solenoid is turned on. The Gedanken experiment measures the change of the interference pattern between cases (a) and (b).

Let us discuss what results we expect to find in this scenario, based on our knowledge of the Aharonov-Bohm effect and the numerical calculation of the propagator. Firstly, let $h$ be large compared to the de Broglie wavelength $\lambda$. When $h$ is large, the Aharonov-Bohm propagator and the semiclassical propagator coincide. Then as in the Aharonov-Bohm experiment, the wave function of an electron experiences a change of phase, given by Eq. (21). However, the phase change of the interference amplitude, given by Eq. (22), now has the outcome $\Delta\delta=0$, because there is no magnetic flux through the region $S$ (between the classical trajectories). Thus switching off and on the magnetic field will not produce a change in the interference pattern.

Now suppose the solenoid approaches the classical trajectory $A-D$, but we assume that its distance from the other classical trajectory $B-D$ is still large. Then the propagator corresponding to the trajectory $A-D$ is given by the Aharonov-Bohm propagator, while the propagator corresponding to the trajectory $B-D$ is given by the semiclassical propagator. Our previous numerical results show a marked difference between the Aharonov-Bohm propagator and the semiclassical propagator (for propagation between the same points). There is a difference not only in phase, but also in modulus. Thus we expect for the interference experiment, when $h$ becomes small and when the magnetic field is switched on and off, that a change of phase as well as of

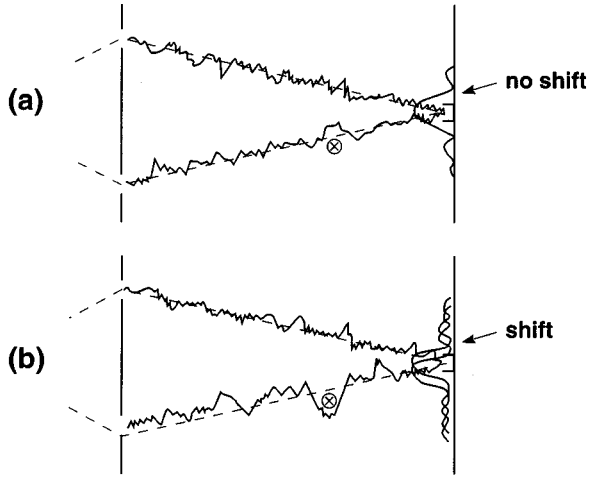


FIG. 12. Gedanken experiment I, similar to Fig. 11. Sketch of interference pattern if there were only two contributing quantum-mechanical paths (in the neighborhood of the two classical paths). If the solenoid is situated outside of the region bounded by the two quantum paths, there is no shift in interference (a), otherwise there is a shift (b).

modulus will show up in the interference amplitude. Its interpretation is as follows: Quantum mechanics, expressed in the language of path integrals, tells us that there are contributions from all possible paths. There are paths close to the classical path (see Fig. 12) that give dominant contributions. There are paths far away from the classical path that give very small contributions. There are also paths crossing the area of the solenoid (in the case of finite extension). As long as all paths of propagation between slit $A$ and detector $D$ pass by the same side of the solenoid [see Figs. 11 and 12(a)], there will be zero change in phase and modulus in the interference amplitude. But when paths occur, which pass on both sides of the solenoid [Fig. 12(b)], or eventually wind around the solenoid as quantum mechanics predicts, then interference is described by the Aharonov-Bohm propagator for route $A-D$ and by the semiclassical propagator for the route $B-D$, producing a change of the interference pattern. In other words, any difference between the interference patterns for magnetic fields $\vec{B}=0$ and $\vec{B}\neq 0$ indicates that there must be contributions from paths that have deviated from the classical path $A-D$ by at least a distance $h$. Thus the proposal of experiment I is as follows: (1) Measure the interference pattern when $\vec{B}=0$. (2) Measure the interference pattern when $\vec{B}\neq 0$, as a function of $h$. Any difference between (1) and (2) signals that quantum paths have fluctuated at least by a distance $h$ from the classical trajectory.

In Figs. 9 and 10 we have presented results in dimensionless units. Now we want to take a look at the behavior of the propagator for a more physical choice of parameters. We take $\hbar=c=1$, thus $\hbar c=197$ MeV fm$=1$, and express every quantity in (powers of) fm. The electron mass is $\mu_e=0.511$ MeV$/c^2=0.259\times 10^{-2}$ fm$^{-1}$. We choose $L=2$ cm$=2\times 10^{13}$ fm, $T=1$ s$=3\times 10^{23}$ fm. The diameter of an elementary solenoid used in an Aharonov-Bohm experiment is of the order of $d_{\mathrm{sol}}\sim 5$ $\mu$m$=5\times 10^{9}$ fm. We have varied $h$ from $h=d_{\mathrm{sol}}=5\times 10^{9}$ fm to $h=100d_{\mathrm{sol}}=5\times 10^{11}$ fm. This set of parameters corresponds to a de Broglie wavelength

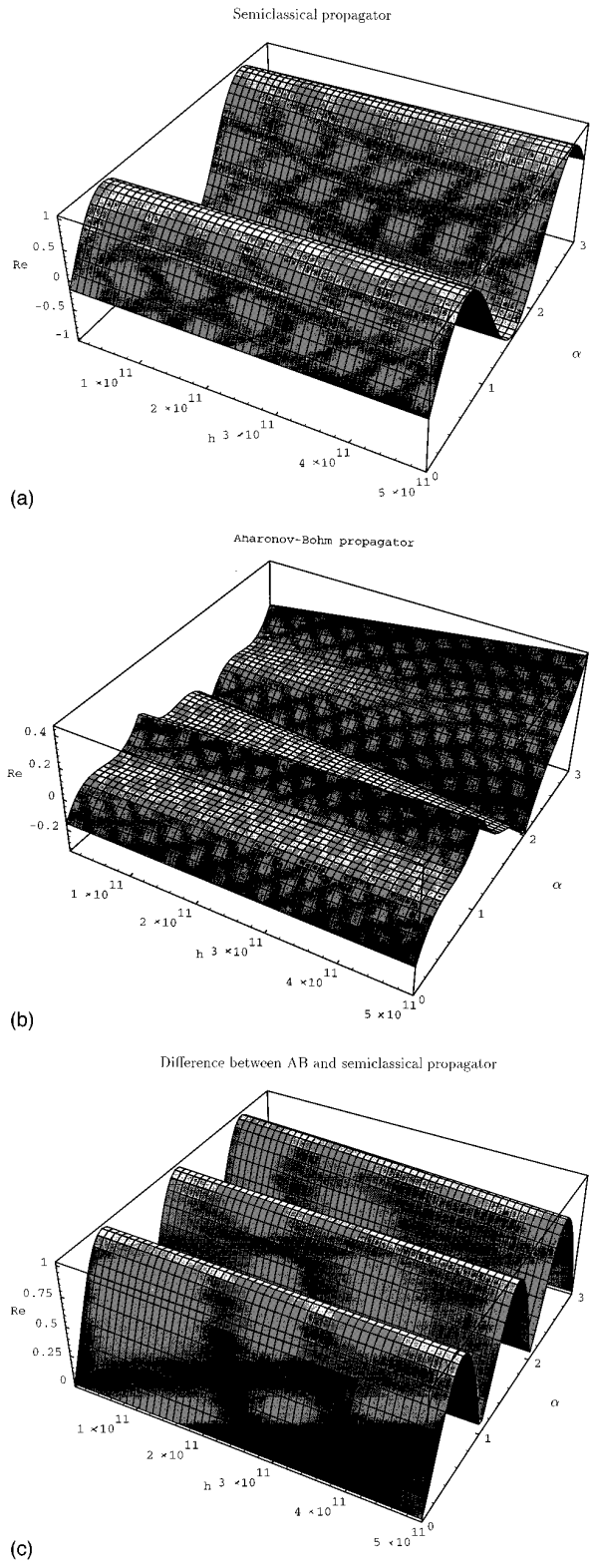


FIG. 13. Same as Fig. 9, after division by factor $\mu/2\pi i\hbar T$. For physical parameters see text.

$\lambda=3.63\times10^{13}$ fm. If we again identify $h=\Delta x$, then we have $2\pi\Delta x/\lambda=0.86\times10^{-3}$ for $h=d_{\rm sol}$ and $2\pi\Delta x/\lambda=0.86\times10^{-1}$ for $h=100d_{\rm sol}$. Thus we are in the quantum-mechanical region. Experimentally, the magnetic flux can be varied continuously in a certain range [15]. Dirac's quantization condition of flux from a Dirac string attached to a magnetic monopole is given by [16] $q\phi/2\pi\hbar c=\alpha=n$, $n=0,1,2,\ldots$ Thus it is reasonable to vary $\alpha$ in the order of unity. We have varied $\alpha$ from 0 to 3. We have plotted the propagators after dividing by the common factor $\mu/2\pi i\hbar T$. Figure 13(a) displays the real part of the semiclassical propagator; Fig. 13(b) shows the real part of the Aharonov-Bohm propagator, and in Fig. 13(c) we have plotted the absolute value of the real part of their difference. Figure 13(c) shows that when the solenoid has a distance from the classical trajectory in the order of several $d_{\rm sol}$, there is a marked difference in particular for $\alpha\approx1/2,3/2,\ldots$, i.e., half integer. This quantum-mechanical effect should be observable experimentally.

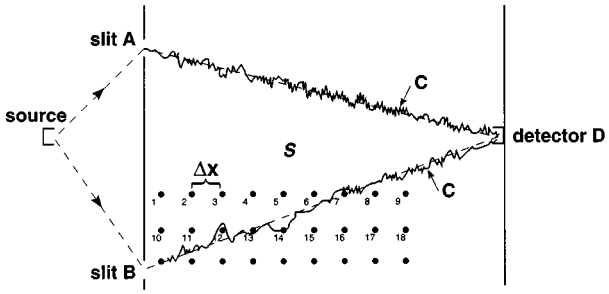


FIG. 14. Setup of Gedanken experiment II. Same as Gedanken experiment I, but there are many solenoids.

Summarizing this section, a change in the interference pattern can only occur due to contributions of paths, which aberrate from the classical path, in such a way that the solenoid is in the interior of the region bounded by the two paths (coming from the two slits). Thus the observation of a change of the interference pattern in this Gedanken experiment shows directly the necessity to take into account contributions from paths aberrating from the classical path. But it does not necessarily show that the paths zigzag. The aberration could be a smooth one like a sin curve. In order to get more information on the geometry of those paths, in particular on average length, scaling behavior, critical exponent, i.e., Hausdorff dimension, we suggest another Gedanken experiment.

## VI. GEDANKEN EXPERIMENT II TO MEASURE THE FRACTAL DIMENSION OF QUANTUM-MECHANICAL TRAJECTORIES

### A. Setup

This setup is a generalization of the setup of Gedanken experiment I. As discussed above, one needs an elementary length scale $\Delta x$ and one has to measure the length of the trajectory in terms of this elementary length scale. I suggest taking as an elementary length scale the distance between two neighboring solenoids in an array of solenoids (see Fig. 14). The array of solenoids is placed such that the classical trajectory coming from slit $A$ passes through this array, while the classical trajectory coming from the slit $B$ does not pass through this array. For example, the array could be placed in the lower half plane bounded by a line of points that are equidistant from the two slits.

As pointed out above, analytical and numerical calculations have given Hausdorff dimension $d_H=2$ for free

quantum-mechanical motion. This is valid for motion in $D=1,2,3$ space dimensions. In this sense the trajectory shown in Fig. 3 is not quite correct: The motion zigzags in the longitudinal as well as the transversal direction, while in Fig. 3 zigzagness is shown only in the transversal direction. This experiment will be sensitive only to zigzagness in the plane perpendicular to the flux tubes. The reason is as follows: The massive charged particle interacts with the vector potential corresponding to the magnetic field of the solenoids. The solenoids represent (idealized) infinitely long and thin flux tubes. The system is invariant with respect to translations parallel to the flux tubes. Any zigzagness of motion in this direction does not show up in the phase factor $\exp[iq/\hbar c\int_C d\vec{x}\cdot\vec{A}]$ and hence does not show up in the interference pattern.

From Gedanken experiment I we have learned that observable quantum effects occur when quantum paths deviate from the classical path such that quantum paths go by both sides of the solenoid. As a consequence, this experiment is sensitive only to zigzagness on a length scale larger than the minimal distance between two solenoids i.e., $\Delta x$. This is due to the topological character of our experiment. Thus we ask: What are the topologically different (homotopy) classes of paths, corresponding to the given geometry of selonoids assuming we have $N_S$ solenoids positioned in a regular array with next-neighbor distance $\Delta x$? The topological class of a path depends on the starting point $x_{\text{in}}$, the endpoint $x_{\text{fin}}$, and the way it winds around the individual solenoids. One should note that this does not depend on the sequential order of winding around individual solenoids. Equivalent paths with the same winding but different sequential order are shown in Fig. 15. Mathematically, this is characterized by the phase factor $\exp[iq/\hbar c\int_C d\vec{x}\cdot\vec{A}]$, corresponding to the path $C$. If, e.g., the path $C$ is closed and winds around solenoids $1,\ldots,N_S$, respectively, with winding numbers $n_1,\ldots,n_{N_S}$, this phase factor yields

$$\exp\left[\frac{iq}{\hbar c}\left[n_1\phi_1+\cdots n n_{N_S}\phi_{N_S}\right]\right]. \tag{33}$$

From the knowledge of this phase factor one can extract the winding numbers of solenoids in a unique way, if the flux values $\phi_1$ to $\phi_k$ are incommensurable, i.e., their ratios are not rational numbers. In practice, however, quantum effects in the amplitude due to high winding numbers become very small and eventually for $n_w$ larger than some cutoff $n_{\text{cutoff}}$ they are no longer detectable in an experiment. Thus we can allow the ratio of fluxes

$$\frac{\phi_i}{\phi_j}=\frac{n_i}{n_j},\quad n_i,n_j>n_{\text{cutoff}} \tag{34}$$

The experiment consists of measuring the interference pattern, once when all solenoids are turned off and once when all solenoids are turned on. Any change in the interference pattern is due to a change of wave function, that traverses the array of solenoids. How is the change of the phase and modulus of the wave function related to the flux of the solenoids? This is answered by the rules of quantum mechanics expressed in terms of the path integral: The wave function is given by the path integral

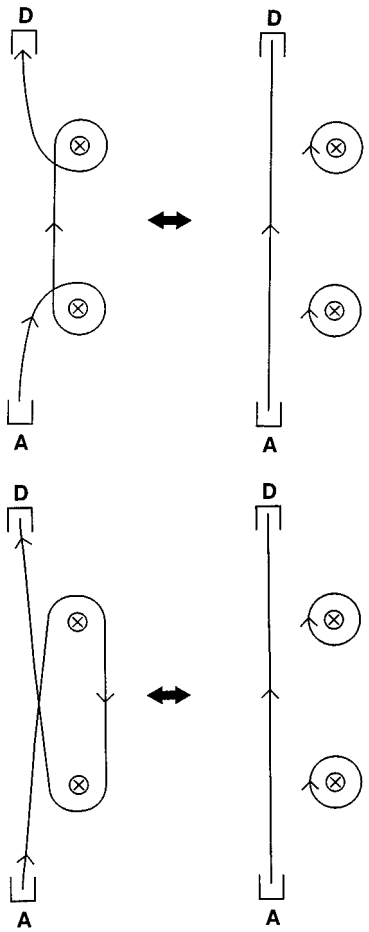


FIG. 15. Topologically equivalent paths.

$$\psi(\vec{x},t)=\int [dx]\exp(i/\hbar S[\vec{x}])|_{\vec{x},t;\vec{x}_0,t_0}, \tag{35}$$

representing all paths between $\vec{x}_0,t_0$ and $\vec{x},t$. For the purpose of the interference experiment one would choose $\vec{x}_0,t_0$ corresponding to the source and $\vec{x},t$ corresponding to the detector. All paths go through either one of the two slits. The integral is a sum over paths. By splitting the action into a kinetic and a magnetic part the wave function can be expressed as

$$\psi(\vec{w},t)=\sum_C \exp i/\hbar S_{\text{free}}[C] \times\exp\left[\frac{iq}{\hbar c}\int_C d\vec{x}\cdot\vec{A}(\vec{x},t)\right]\Bigg|_{\vec{x},t;\vec{x}_0,t_0}. \tag{36}$$

The wave function is a superposition of phase factors. Each phase factor has been split into a term representing the weight of the free action and a term representing the phase of a line integral of the vector potential. If we would retain in Eq. (36) only one path $C_1$ passing through slit 1 and one path $C_2$ passing through slit 2 (which is of course unphysical), then the interference pattern, given by the absolute amplitude squared, would be determined by the difference of the phases corresponding to $C_1$ and $C_2$ (see Ref. [12]). But the difference of two line integrals, both going from $\vec{x}_0,t_0$ to $\vec{x},t$,

corresponds to a line integral along a closed curve $C$ (following $C_1$ and returning by $C_2$). Then the second phase factor in Eq. (36) would describe the total flux going through the area $S$ interior to $C$, as given in Eqs. (21) and (22).

### B. Reconstruction of paths: case of two paths

The Gedanken experiment measures the interference pattern and hence the change of the phase and modulus of the wave function. The question is how to extract from this information about the geometry of paths, and in particular about the length of the average path. We want to treat this problem in two steps: Firstly, suppose there is only one path corresponding to each slit. The shift of the phase $\Delta\delta$ of the wave function is then given by the sum of fluxes of the solenoids in the interior area $S$. In Fig. 14, those are the fluxes of solenoids 1 to 6, 10, 11, 13, and 14. Suppose we know the shift $\Delta\delta$ and hence the total flux. How can we tell from that which particular solenoids have contributed to the flux? This information is necessary in order to trace the trajectory. It can be answered in the following way: We must assign to each solenoid a particular flux, such that knowing the total flux allows one to reconstruct which individual fluxes have contributed. This is certainly not possible when all individual fluxes have the same value. This problem is mathematically equivalent to the following problem in number theory: Given is a finite set of real numbers $r_i$, $i=1,\ldots,N$, and a real number $R$. Suppose we know that the equation

$$n_1 r_1 + \cdots n_N r_N = R \tag{37}$$

possesses a solution for a set of integer numbers $n_1,\ldots,n_N$. We want to know the following: Under what conditions is this solution unique? A possible answer is the following: One chooses $r_i$, $i=1,\ldots,N$ as the ratio of large integer numbers, which do not possess a common integer divisor. One imposes a cutoff on the integer numbers $n_i < n_{\text{cutoff}}$, where $n_{\text{cutoff}}$ is small compared to the integers occurring in the numerators and denominators of $r_i$. Then the solution is unique. Let us give an example: $r_1=97/99$, $r_2=101/111$, $R=8463/10989$. Then

$$\frac{8463}{10989} = n_1 \frac{97}{99} + n_2 \frac{101}{111} \tag{38}$$

possesses the solution $n_1=-2$, $n_2=3$, but no other integer solution for say $-3<n_i<3$.

Here we have made the following association between the integer numbers and our experiment:

$$R \leftrightarrow \text{total flux},$$

$$r_j = \leftrightarrow \text{flux of individual solenoid } j,$$

$$n_j = \leftrightarrow \text{winding number of path around solenoid } j. \tag{39}$$

Suppose we have tuned the magnetic field of the individual solenoid $j$, such that the corresponding individual flux takes on the value $r_j$. From the experiment we know the total flux $R$. Thus we can determine in a unique way the winding numbers $n_j$.

### C. Reconstruction of paths: case of many paths

The above procedure allows one to reconstruct the path, if there is a single path. In quantum mechanics there are infinitely many paths that contribute to the amplitude. How can we reconstruct the average path from the knowledge of the interference pattern in the general case? The idea is to take advantage of the connection between quantum mechanics and topology. Recall the discussion of the Aharonov-Bohm effect: The quantum-mechanical free propagator can be written as a decomposition of the free propagator into winding number sectors and then summing over all winding numbers [Eq. (28)]. The Aharonov-Bohm propagator has a similar decomposition. However, now the contribution from a given winding sector is the product of the free propagator in this winding sector times the Aharonov-Bohm phase factor $\exp[i\alpha(\theta'-\theta+2\pi n_w)]$ [Eq. (31)]. One aspect of this is important in the following: If one varies the magnetic flux in the solenoid $\phi \rightarrow \phi'$ and hence $\alpha \rightarrow \alpha'$, this changes of course the total Aharonov-Bohm propagator. It also changes the Aharonov-Bohm phase factor in each winding sector. But it *does not change* the free propagator in each winding sector.

All this carries over to the generalized Aharonov-Bohm setting with the array of $N_S$ solenoids. Again the full propagator decomposes into homotopy classes. The contribution from each homotopy class is the free propagator in this homotopy class times a generalized Aharonov-Bohm phase factor,

$$\exp\left[\frac{iq}{2\pi\hbar c}\{(\theta'-\theta)\phi_{\text{tot}} + 2\pi[n_1\phi_1 + \cdots n_{N_S}\phi_{N_S}]\}\right],$$

$$\phi_{\text{tot}} = \phi_1 + \cdots \phi_{N_S}. \tag{40}$$

The important aspect is again: Changing the fluxes $\phi_i$ changes the full propagator, but does not change the free propagator in each homotopy class.

Thus experimentally, we have a way to determine the free propagator corresponding to a given homotopy class. We introduce a cutoff in the winding numbers $n_i < n_{\text{cutoff}}$. What value would one attribute to $n_{\text{cutoff}}$? In a Gedanken experiment one considers an idealized situation neglecting experimental errors. In such a situation one would consider $n_{\text{cutoff}}$ as a parameter that should be increased until the Hausdorff dimension of the quantum path (Sec. VI) converges. In a more realistic situation one faces experimental errors or more precisely thresholds (limits) of experimental resolution. One expects that winding numbers beyond the cutoff give contributions to the amplitude that are of the order of experimental errors and hence cannot be detected. The relation between a given experimental threshold and the corresponding value of $n_{\text{cutoff}}$ could be estimated via a numerical simulation of the path integral.

This cutoff makes the number of homotopy classes finite. Let us enumerate the homotopy classes by $n_h = 1,2,\ldots,N_H$. The experimenter chooses a set of fluxes of the solenoids:

$\phi_i^{(1)}$, $i=1,\ldots,N_S$. Then he measures the corresponding interference pattern, say $I^{(1)}$. Then the experimenter chooses another set of fluxes of the solenoids, $\phi_i^{(2)}$, $i=1,\ldots,N_S$, and measures again the interference pattern, $I^{(2)}$. This is repeated for $N_F$ different sets of fluxes. The gathered information is then sufficient to determine the free propagators in the homotopy classes $n_h=1,\ldots,N_H$. The wave function for emission from the source at $\vec{x}_0,t_0$ is given by

$$\psi(\vec{x},t)=\sum_C \exp i/\hbar S_{\text{free}}[C]\exp\left[\frac{iq}{\hbar c}\int_C d\vec{x}\cdot\vec{A}(\vec{x},t)\right]\Bigg|_{\vec{x},t;\vec{x}_0,t_0}$$

$$=\sum_{n_h} K_{n_h}^{\text{free}}\exp\left[\frac{iq}{2\pi\hbar c}\{(\theta'-\theta)\phi_{\text{tot}}+2\pi[n_1\phi_1+\cdots n_{N_s}\phi_{N_s}]\}\right]. \tag{41}$$

The interference pattern is given by the squared modulus of the wave function

$$I=|\psi(\vec{x},t)|^2. \tag{42}$$

Thus considering $N_F$ different sets of fluxes, one has

$$I^{(f)}=\left|\sum_{n_h} K_{n_h}^{\text{free}}\exp\left[\frac{iq}{2\pi\hbar c}[(\theta'-\theta)\phi_{\text{tot}}^{(f)}+2\pi(n_1\phi_1^{(f)}+\cdots n_{N_s}\phi_{N_s}^{(f)})]\right]\right|^2, \quad f=1,\ldots,N_F. \tag{43}$$

Because a given set of fluxes and a given homotopy class $n_h$ determines the generalized Aharonov-Bohm phase factor, and the free propagator in each homotopy class $K_{n_h}^{\text{free}}$ is independent of the fluxes, this equation allows one to determine the unknown coefficients $K_{n_h}^{\text{free}}$, $n_h=1,\ldots,N_H$. Because $K_{n_h}^{\text{free}}$ are complex numbers, and the fluxes $\phi$ and vector potentials $\vec{A}$ are real, we need at least twice as many sets of fluxes as the number $N_H$ of homotopy classes considered, $N_F>2N_H$.

### D. Length of paths

Suppose we know by now from experiment the values of $K_{n_h}^{\text{free}}$ corresponding to a given homotopy class $n_h$. What length of path would we assign to it? Consider the array of solenoids with distance $\Delta x$ between neighboring solenoids. Homotopy classes are distinguished by the phase factor of the vector potential $\exp[iq/\hbar c\int_C d\vec{x}\cdot\vec{A}]$. We start by grouping paths occurring in the path integral, Eq. (36), into classes: Two paths are in the same class, if they can be made identical by stretching and deforming without crossing a solenoid. This reflects the fact that we cannot resolve any structure on a scale smaller than the resolution $\Delta x$. Moreover, the phase factor of the vector potential does not distinguish the paths, such as, e.g., in Figs. 15(a) and 15(b). These two paths belong to the same class. These two paths can be transformed into each other by deformation of paths and applying the following rule: When two oriented paths cross each other, they can be cut at the vertex such that each each piece has an incoming and an outgoing line relative to the vertex. For each class we define a representative path, which passes in the middle between two neighboring solenoids. Then one draws a straight line from the middle of one of those pairs to the middle of the next of those pairs (see Fig. 16). Each of those representative paths is defined by a given sequence of pairs of solenoids. What representative path do we associate, e.g., to those topologically equivalent paths of Figs. 15(a) and 15(b)? Because the length of the curve is expected to go to infinity, when $\Delta x\to 0$, we are experimentally on the conservative side, if we choose the shortest path from those of Figs. 15(a) and 15(b), that is, the path that goes forward in the longitudinal direction, except for loops around individual solenoids (this is shorter than doing one loop around two solenoids). Thus the rule for representative path is as follows: It starts at $x_{\text{in}}$ and arrives at $x_{\text{fin}}$. It goes by pieces of straight lines always passing in the middle of a pair of solenoids. The representative path is determined by the winding numbers corresponding to the solenoids of the array. Among several paths compatible with the same winding numbers, the shortest path is taken as the representative path. That means that each loop goes around at most one solenoid (possibly several times). An example of such a path is shown in Fig. 16. In this sense, we associate to each homotopy class a representative path. Let us denote those representative paths by $C_r$. Then we define the classical length of the trajectory as follows:

$$L_{C_r}(\Delta x)=\text{sum of length of pieces of straight line.} \tag{44}$$

Finally, we want to obtain a quantum-mechanical expression

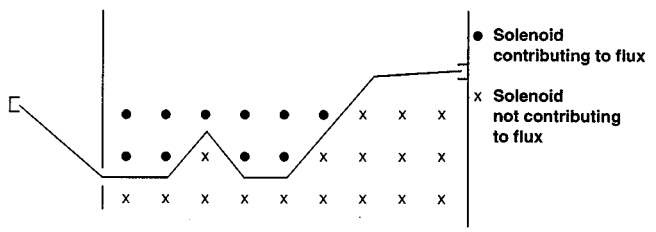


FIG. 16. Gedanken experiment II. Prescription how to associate a length to a particular quantum path corresponding to Fig. 14.

for the length of paths. The general expression is a weighted average given by the transition element

$$\langle L\rangle = \frac{\sum_C L_C \exp\{iS[C]/\hbar\}}{\sum_C \exp\{iS[C]/\hbar\}}, \tag{45}$$

where the sum goes over all possible paths $C$ that go from the source at $t_{\rm in}$ to the detector at $t_{\rm fin}$. This is meant to be the same length definition as given in Eq. (15), but taking $N\to\infty$ and introducing a normalizing factor. In the discussion of experiment II we have introduced an elementary length scale $\Delta x$. In order to obtain an operational length definition for the experiment, we replace the infinite sum over all paths in Eq. (45) by a finite sum over the representative paths and the weight factor $\exp[iS/\hbar]$ is given by the action in the homotopy class corresponding to the representative path. Thus we obtain

$$\langle L(\Delta x)\rangle = \frac{\sum_{C_r} L_{C_r} \exp\{iS[n_h]/\hbar\}}{\sum_{C_r} \exp\{iS[n_h]/\hbar\}}, \tag{46}$$

where

$$\exp\{iS[n_h]/\hbar\} = K^{\rm free}_{n_h}\exp\left[\frac{iq}{2\pi\hbar c}\{(\theta'-\theta)\phi_{\rm tot} + 2\pi[n_1\phi_1+\cdots n_{N_s}\phi_{N_s}]\}\right], \tag{47}$$

and $K^{\rm free}_{n_h}$ has been determined from our experiment. This yields $\langle L\rangle$ for a given array of solenoids, characterized by $\Delta x$, in the presence of the vector potential of the solenoids. But we can also obtain the length in the absence of the vector potential, i.e., corresponding to free propagation: The length is still given by Eq. (46). But the action weight factor, putting all fluxes $\phi_i\equiv 0$, is then

$$\exp\{iS[n_h]/\hbar\} = K^{\rm free}_{n_h}. \tag{48}$$

Finally, in order to extract the Hausdorff dimension $d_H$, we have to measure the length $\langle L(\Delta x)\rangle$ for many values of $\Delta x$, look for a power law behavior when $\Delta x\to 0$, and determine the critical exponent and thus $d_H$.

At the end of this section we discuss limitations and errors. As a consequence of the fact that this experiment is not sensitive to the zigzagness parallel to the solenoids, we do not measure the length of the path but only its projection onto the plane perpendicular to the solenoids, i.e., in $D=2$ dimensions. Nevertheless, the length as such is physically not so interesting (it depends on $\Delta x$ anyway). The physically important quantity is the critical exponent (Hausdorff dimension), which corresponds to taking the limit $\Delta x\to 0$. But the latter should be the same in any space dimension.

Let us comment on the two length definitions employed here: Firstly, there is the general definition, Eq. (45) expressed as a path integral. Secondly, there is an operational definition Eq. (46) proposed to be applied in the experiment. These definitions differ in two aspects: (i) While Eq. (45) describes the continuum limit and takes into account infinitely many paths, Eq. (46) is an approximation, taking into account only a finite number of paths. This is the same kind of approximation as is done when replacing an ordinary integral by a finite sum. When letting $\Delta x$ go to zero, the number of paths tends to infinity. (ii) The more serious difference is the fact that while Eq. (45) represents all paths, Eq. (46) chooses only one representative path for each homotopy class, although there may be several topologically inequivalent paths in the same homotopy class. An example is shown in Fig. 15.

Finally, let us suppose the experiment were performed and the experimenters would have extracted $d_H=1.5\pm 0.1$. What would one conclude from this? Firstly, such a result would establish that quantum paths are fractals (anything with $d_H>1$). But then one would ask the following: For theoretical reasons, would one expect to find $d_H=2$. What is the reason for this difference? As pointed out above, the theoretical result $d_H=2$ is not rigorously established. Thus it may be that $d_H=1.5$ is the correct answer and $d_H=2$ is wrong. However, this is quite unlikely. Nevertheless, it is very desirable to get a firm theoretical answer. This could be done by proving Eq. (13) or at least by solving the path integral by computer simulation in real time and extracting $d_H=2$. Suppose the latter had been achieved. Then one would conclude that the proposed experiment is incomplete, in the following sense: It shows that quantum paths zigzag, but the experiment ''does not capture all zigzagness.'' Possible errors are as follows: (a) The upper limit of winding number imposed in the experiment is too small. (b) The distance between solenoids $\Delta x$ is too large. (c) The chosen definition of representative path in a given homotopy class, namely the shortest connected path among topologically inequivalent paths within a homotopy class, is incorrect. Errors (a) and (b) are questions of experimental precision, which may be a substantial problem when doing a real experiment. However, we do not consider it a serious conceptual problem (in a Gedanken experiment). The most serious point and possibly the weakest part in our view is (c). If the definition of the representative path is incomplete, one cannot test quantum mechanics. In order to verify the proposed length definition of a representative path, we suggest doing a numerical simulation of path integrals in the presence of the solenoids and computing the quantum-mechanical length as defined by Eq. (46) with that defined by Eq. (45).

## VII. SUMMARY

We have made a proposal of how to observe experimentally the zigzag motion of quantum-mechanical paths. We have suggested two experiments: Experiment I is conceived to show the existence of zigzagness. Experiment II is conceived to determine the average length of path, its scaling behavior when $\Delta x\to 0$, and eventually the corresponding Hausdorff dimension. Finally we want to return to the Heisenberg uncertainty principle, as discussed in Sec. III in the context of the multislit experiments. It says the following: The higher the precision in measuring positions to determine a quantum path, the more it will change the interfer-

ence pattern of the quantum amplitude. What relevance does this have to our experiment? What does our experiment have in common with the multislit experiment of Sec. III? Where does it differ? Firstly, in the multislit experiment the spatial resolution is given by the distance between holes and the wavelength of light. In our experiment the spatial resolution is given by the distance between solenoids. Thus the array of multiple screens with multiple holes corresponds to the array of solenoids. This is a common feature between our experiment and the multislit experiment. However, the rest is different: In the multislit experiment, by interaction with light, one determines the holes passed by the electron, but at the same time modifies its quantum path and hence its interference pattern. In our experiment, for each set of solenoids with a given set of fluxes, corresponding to time-independent vector potentials, one does not measure the position, but the undisturbed interference pattern of the electron propagating in the vector potential. Then one changes the set of fluxes (but not the position of solenoids), and measures again the interference pattern. This is repeated a number of times. The crucial point is this: Changing the fluxes of the solenoids (and hence the vector potential) does not change the free propagator in the homotopy class given by the array of solenoids. Thus measuring the interference pattern for a large enough number of sets of different fluxes allows to determine the free propagator in the homotopy classes. From that follows the length. Thus contrary to the multislit experiment, we do not determine the holes (or pairs of solenoids) that the electron has passed, but relative amplitudes for classes of quantum-mechanical paths.

Finally, let us comment on the practical feasibility of our proposed experiments. Certainly experiment I is much simpler. Assuming the diameter of a realistic small solenoid to be of the order of $d_{\mathrm{sol}}=5\ \mu$m, we have seen that quantum-mechanical effects should be clearly observable when the solenoid is placed in a wide range of distances (e.g., $h=d_{\mathrm{sol}}$ to $h=100d_{\mathrm{sol}}$ for the particular choice of the parameters) from the classical trajectory, provided that the flux is such that $\alpha$ takes values in the neighborhood of half integer numbers. The second experiment is more difficult. However, part of the experiment can be tested by comparison with theory: For the case of one single solenoid, the homotopy classes and the free propagator in each homotopy class are known analytically. This can be compared with the results of the experiment.

## ACKNOWLEDGMENTS

The author is grateful for discussions with Professor Franson, Johns Hopkins University, Professor Pritchard, MIT, Professor Cohen-Tannoudji, Ecole Normale Supérieure, and Professor Hasselbach, Universität Tübingen. The author is grateful for support by NSERC Canada.

[1] R. P. Feynman and A. R. Hibbs, *Quantum Mechanics and Path Integrals* (McGraw-Hill, New York, 1965).
[2] B. B. Mandelbrot, *The Fractal Geometry of Nature* (Freeman, New York, 1983).
[3] L. F. Abbot and M. B. Wise, Am. J. Phys. **49**, 37 (1981).
[4] E. Campesino-Romeo, J. C. D'Olivio, and M. Sokolovsky, Phys. Lett. A **89**, 321 (1982).
[5] R. P. Feynman and A. R. Hibbs, *Quantum Mechanics and Path Integrals* (Ref. [1]), Secs. 7.2 and 7.3.
[6] H. Kröger, S. Lantagne, K. J. M. Moriarty, and B. Plache, Phys. Lett. A **199**, 299 (1995).
[7] O. Madelung, *Solid State Theory* (Springer, Berlin, 1981).
[8] K. A. Brueckner, Phys. Rev. **97**, 1353 (1955).
[9] Y. Aharonov and D. Bohm, Phys. Rev. **115**, 485 (1959).
[10] F. Wilczek, *Fractional Statistics and Anyon Superconductivity* (World Scientific, Singapore, 1990).
[11] F. G. Werner and D. R. Brill, Phys. Rev. Lett. **4**, 344 (1960), see references therein.
[12] R. P. Feynman, R. B. Leighton, and M. Sands, *The Feynman Lectures on Physics* (Addison-Wesley, Reading, 1964), Vol. II.
[13] L. S. Schulman, J. Math. Phys. **12**, 304 (1971).
[14] L. S. Schulman, *Techniques and Application of Path Integration* (Wiley, New York, 1981).
[15] A. Tonomura, H. Umezaki, T. Matsuda, N. Osakabe, J. Endo, and Y. Sugita, Phys. Rev. Lett. **51**, 331 (1983), see references therein.
[16] T. P. Chen, L. F. Li, *Gauge Theory of Elementary Particle Physics* (Oxford University Press, Oxford, 1984).